CMS TN 94 - 136
January 1994

The Micro-Strip Gas Chamber behaviour in a magnetic field

F.Angelini[5], R.Bellazzini[5], M.Bozzo[3], A.Brez[5], J.F.Clergeau[4], D.Contardo[4], A.Markou[1], M.M.Massai[5], T.Meyer[2], R.Raffo[5], R.Ribeiro[2], G.Smadja[4], G.Spandre[5], M.Spezziga[5]

(1) Demokritos Athens,(2) CERN, (3) INFN Genova, (4) IPN Lyon, (5) INFN Pisa

ABSTRACT

A Micro Gap Chamber and two Micro-Strip Gas Chambers have been tested in the RD5 magnet at the CERN-SPS with a 300GeV/c muon beam. The results of an analogical and logical analysis of the data are presented.

I Experimental set-up

The overall RD5 experimental set-up is shown in figure 1 and the geometry of the chamber telescope is presented in figure 2. The chambers provided by the Pisa group have an anode pitch of 200μm and a gas gap of 3mm. The widths of anodes (cathodes) are 5(200)μm in the MGC[1] and 9(60) in the MSGC[2]. The voltages applied to the cathodes and to the drift plan of each counters are summarized in table 1, together with the corresponding drift fields[3].

The read-out was performed with the Laben preamplifiers and amplifiers used by Pisa in the NA12 experiment. For a minimum ionizing particle, the rise time of the signal is 10ns and the FWHM is 50ns. The integrated charge was measured with ADC modules. The width of the gate was 200ns leading to a signal to noise ratio of 10, where the signal is defined as the energy loss of maximum probability for a minimum ionising particle and the noise is the mean RMS value of the ADC pedestals.

The recorded data include measurements as a function of :

- The magnetic field, up to B=2.24T.
- The tilt angle of the detectors (α_T) referenced as the Lorentz angle (α_L) (fig.2b).
- The gas mixture, Ar/DME (80/20%), DME/CO_2 (70/30%) and DME/CF_4 (87/13%).

II Analysis procedure

Two analyses, logical and analogical, are presented. The position of a detected particle is estimated from the center of gravity of the excited strips. In the analogical analysis, the ADC amplitudes are used to weight the position of the strips. In the logical analysis, all the strips with a signal above the threshold have the same spatial weight, this is equivalent to the situation with a digital read-out.

a) Alignment of the detectors

For each gas mixture the 3 chambers were aligned to the RD5 Si-hodoscope at B = 0 so that the difference in the vertical position, y_{ch}-y_{Si}, is zero when the chambers are perpendicular to the beam (α_T=0).

Gas mixture	E_{drift}(kV/cm)	MGC(V)	MSGC2(V)	MSGC3(V)
Ar/DME	7.1	380	575	580
		2600	2500	2650
	8.2	380	575	580
		2950	2850	3000
	9.0	380	575	580
		3200	3075	3250
DME/CO_2	8.8	450	700	680
		3200	3075	3250
	10.	450	700	680
		3550	3450	3650
DME/CF_4	10.	450	700	700
		3550	3450	3650

Table 1 : Drift field, cathode voltages (smaller value) and drift voltages applied to the detectors.

b) Cluster selection

- Analogical analysis :

In this analysis, we apply a first threshold 2σ above the mean value of the ADC pedestal on each channel content. This reduces the random noise occupancy of the total number of strips to a level of 2%. All the adjacent strips with a signal above the first threshold are considered to belong to a cluster. The amplitude of the cluster is given by the sum of the individual signals. Only the clusters with an amplitude above a second level threshold are selected as candidates for the tracks definition. The efficiency (defined below) and the noise occupation of the second chamber were studied as a function of this threshold (fig.3). We chose a value at 3σ above each mean ADC pedestal, which reduces the noise level to 0.5% of the number of strips, while the efficiency is still maximum. The position associated to a cluster is the center of gravity of the individual signals.

- Logical analysis :

The ADC amplitude of each strip is set to 1 above the threshold and to 0 below. A cluster is defined by the adjacent strips with amplitude 1, no further threshold can be applied in this case. The position is given by the center of gravity method with weight 1 for each strip of the cluster.

As in the case of the analogical analysis, we chose the threshold in order to ensure the best efficiency of the detectors while keeping the noise at a reasonable level (fig.4) for each channel, the final threshold above the mean value of the ADC pedestal is 2.5, 2.75 and 3.0 times the corresponding RMS, respectively for the Ar/DME, DME/CO_2 and DME/CF_4 gas mixtures. The noise occupancy remaining after this cut is 0.4% of the number of strips, close to the one obtained in the analogical case. In both analyses, the sharp decrease of the efficiency and of the noise occur around the same value of the threshold, leading to a limited range of choice for this threshold. We did not investigate the influence of the first threshold in the analogical case.

c) Track selection

The definition of a track crossing the telescope is identical for both kind of analyses, it requires :

- A track detected in the Si-hodoscope.

- Two clusters, in chambers i and j respectively, with a position difference y_i-y_j within 3σ of the mean value of the corresponding distribution.

- A cluster in the third chamber with a position difference y_k-y_{th} within 3σ of the mean value of the corresponding distribution. y_{th} being a linear extrapolation of y_i and y_j.

d) Definition of the resolution

The resolution of each chamber is determined from the RMS of the 3 distributions y_i-y_j for the tracks defined above, according to the following formula :

$$\sigma_i = ((\sigma_{ij}^2 + \sigma_{ik}^2 - \sigma_{jk}^2)/2)^{1/2}$$

The effect of the angular dispersion of the beam, as measured by the Si-hodoscope, is quadratically substracted.

e) Definition of the efficiency

The efficiency of chamber k is the ratio of the number of tracks with associated clusters in chambers i,j and k to the number of tracks with associated clusters only in chambers i and j. To estimate the efficiency, the clusters in i and j are considered to define a track if y_i-y_j is within 2σ of the mean value of the distribution. A cluster in chamber k is considered to belong to the same track if y_k-y_{th} is within 3σ of the mean value of the distribution (y_{th} is a linear extrapolation of y_i and y_j).

f) Definition of the Lorentz angle

In the magnetic field, the Lorentz angle is defined according to the geometry of the experimental device by the formula :

$$\alpha_L = \text{arctg}(2(y_3 - y_2 - l_{23}(y_2 - y_1)/l_{12}) /(d_2+d_3))$$

Where, l_{12} and l_{23} are the gaps between the chambers (46 and 50 mm respectively), d_2 and d_3 the gas gaps of the two last chambers (3.0 and 3.2 mm respectively).

III Experimental results

a) Resolution

- Analogical analysis :

At B = 0 and $\alpha_T = 0$ the resolutions are about $40\mu m$ for all the chambers. The results are similar for the various gas mixtures (table 2).

When increasing B at $\alpha_T = 0$ the resolution is degraded up to a factor 3 at B = 2.24T (fig.5). This effect is larger with Ar/DME but an increase in the drift field, which is lower than for the other gas mixtures, might improve the measured resolution by reducing the Lorentz angle (fig.9).

At B = 2.24T, when compensating the magnetic field effect by tilting the chambers, the resolutions recover the measured values at B = 0 (fig.5 and table 2).

The measured resolutions are very sensitive to the distribution of the number of strips per cluster, i.e. to the thresholds applied. The broadening of the cluster profiles, shown in figure 7, is responsible for the loss of resolution when increasing the magnetic field. However, the resolution does not vary smoothly with the cluster width, this may be due to our choice of the threshold at 2σ. An analysis with a threshold at 1.4σ on the individual strips[1] results into a larger mean value of the number of strips per cluster, probably more significant of the real number of hits associated to a muon track. In figure 7 the cluster profiles suggest that differencies in the resolution of the chambers could be due to the choice of a common threshold. Small misalignments in the mechanical device, or occuring when tilting the chambers might also be responsible for the observed fluctuations in the spatial resolution.

When increasing the magnetic field, the observed degradation of the resolution is larger in the third chamber than in the first two. The optimal resolution when tilting this chamber is also shifted by about 1 degree. Both these effects can be explained by a small initial tilt of the chamber, assumed to be zero in this analysis.

- Logical Analysis :

The resolutions are about $10\mu m$ worse than in the analogical case with a similar behaviour as a function of the magnetic field and the tilt angle (fig.6).

Gas mixture		E_{drift}(kV/cm)	MGC(μm)	MSGC2(μm)	MSGC3(μm)
Ar/DME	B=0T, α_T=0	7.1	52	42	45
	B=2.24T,α_T=α_L	9.0	46	38	44
DME/CO_2	B=0T, α_T=0	10.	47	35	34
	B=2.24T,α_T=α_L	8.8	44	34	38
DME/CF_4	B=0T, α_T=0	10.	33	44	42
	B=2.24T,α_T=α_L	10.	33	31	48

Table 2 : Chamber resolutions (μm) at B = 0, α_T=0 and at B=2.24T, α_T=α_L.

b) Lorentz angle

The Lorentz angle increases linearly with the magnetic field up to 2.24T (fig.8). It decreases when increasing the drift field in the MSGC (fig.9). The slope is steeper for the Ar/DME mixture which presents a larger Lorentz angle at low values of the drift field. However, above 9 kV/cm the measured values should be similar for Ar/DME and DME/CO_2. The Lorentz angles for the different gas mixtures are summarized in table 3.

The tilt applied to the chambers to recover the spatial resolutions measured without magnetic field are compatible with these values (fig.5). The slight shift observed for the third chamber is discussed in the preceeding chapter.

c) Efficiencies

The chamber efficiencies depend on the thresholds applied to the individual strip signals and in the case of the analogical analysis also on the cluster amplitude. A good signal to noise ratio is needed to ensure a good efficiency, this is illustrated on the distributions of the signal amplitudes presented in figure 7.

Gas mixture	E_{drift} kV/cm	Lorentz angle degree
Ar/DME	9.0	9.6
DME/CO_2	8.8	9.8
DME/CF_4	10.	9.3

Table 3 : Lorentz angle at B = 2.24T.

The efficiencies measured at B=0 are summarized in table 4. When increasing the magnetic field they tend to decrease, the slope is larger with the lower drift field applied in the case of the Ar/DME gas mixture (fig.10). A tilt of the chambers equivalent to the Lorentz angle compensates the magnetic field effect and allows to recover the measured efficiencies at B = 0 and $\alpha_T = 0$ (table 4). The obtained values are sometimes even better, due to a reduction of the geometrical area of analysis when tilting the chambers. The measured efficiencies are identical whether one uses the analogical or the logical analyses (fig.11).

Gas mixture		E_{drift}(kV/cm)	MGC(%)	MSGC2(%)	MSGC3(%)
Ar/DME	B=0T, α_T=0	7.1	88.5	96.0	95.5
	B=2.24T,α_T=α_L	9.0	89.0	99.0	98.5
DME/CO_2	B=0T, α_T=0	10.	97.0	97.5	99.0
	B=2.24T,α_T=α_L	8.8	98.0	97.5	97.0
DME/CF_4	B=0T, α_T=0	10.	97.5	97.0	99.5
	B=2.24T,α_T=α_L	10.	99.5	99.5	99.5

Table 4 : Chamber efficiencies (%) at B = 0, α_T=0 and at B=2.24T, α_T=α_L.

IV Conclusion

A MGC and two MSGC detectors have been tested in the RD5 magnet. Without magnetic field, the achieved mean resolution was about $40\mu m$ with an efficiency around 98% and a noise occupancy of 0.5%. The performances of the MGC and MSGC counters are similar.

The Lorentz angle increases linearly with the magnetic field up to 9-10° at B = 2.24T, depending on the gas mixture and the drift field applied in the chamber. The smallest slope measured was 4° per Tesla.

When increasing the magnetic field, the resolutions are degraded up to a factor 3 at B = 2.24T, while the efficiencies decrease by a few percent. A tilt of the chambers equal to the Lorentz angle allows to recover both the resolutions and efficiencies measured without the magnetic field.

The performances are similar for the various gas mixtures, provided the voltages applied both to the cathodes and the drift plan are sufficient. To determine the best gas mixture, the time resolution and the efficiency to inclined tracks have to be studied together with the long term operation of the detectors.

With a digital read-out, the chamber performances would be similar apart for a $10\mu m$ deterioration of the spatial resolution.

[1] F.Angelini et al., Nucl. Instr. and Meth. A335(1993) 69
[2] F.Angelini et al., Nucl. Instr. and Meth. A315(1992) 21
[3] F.Angelini et al., submitted to Nucl. Instr. and Meth.

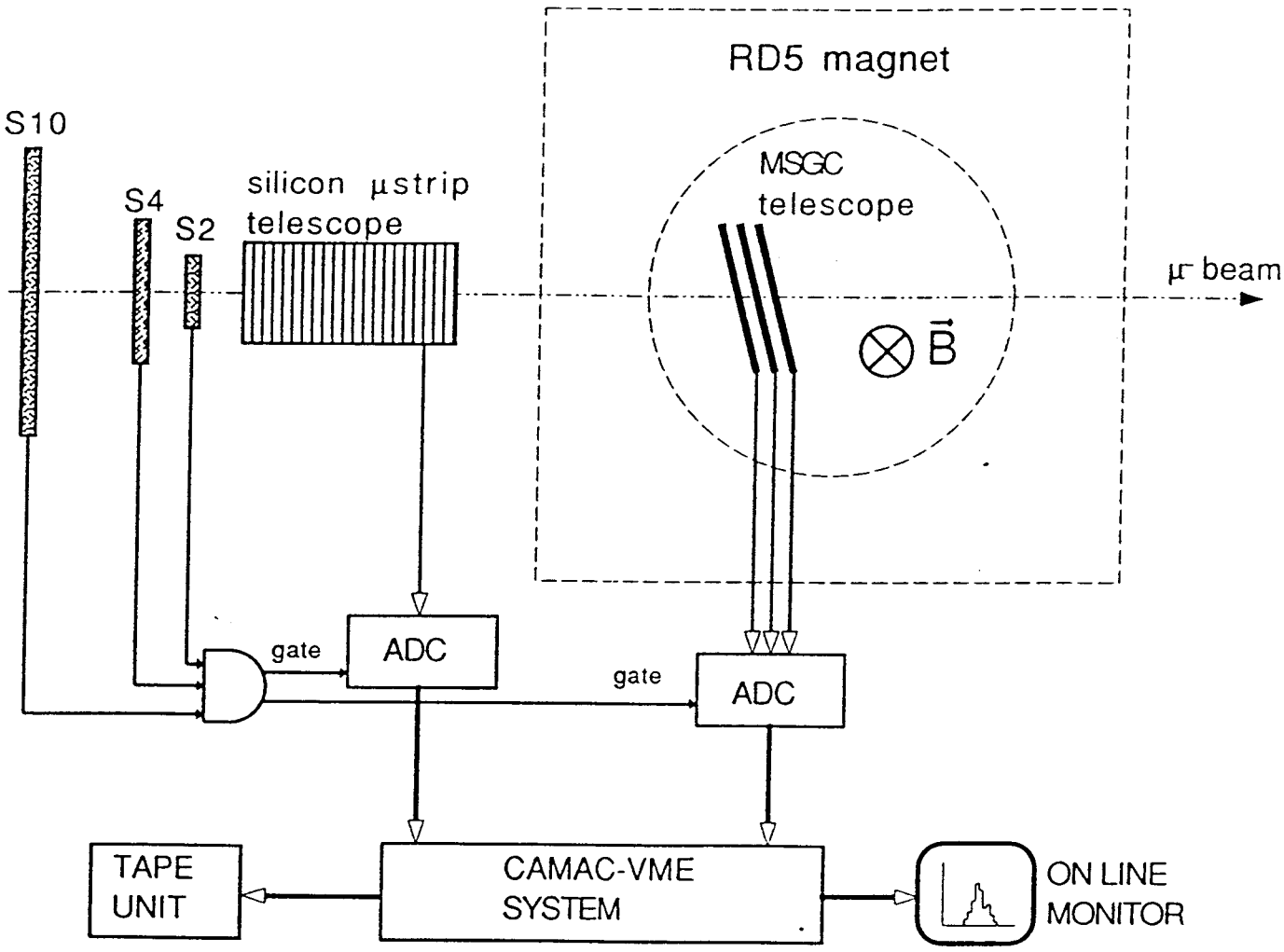

Figure 1 : Schematic view of the experimental set-up.

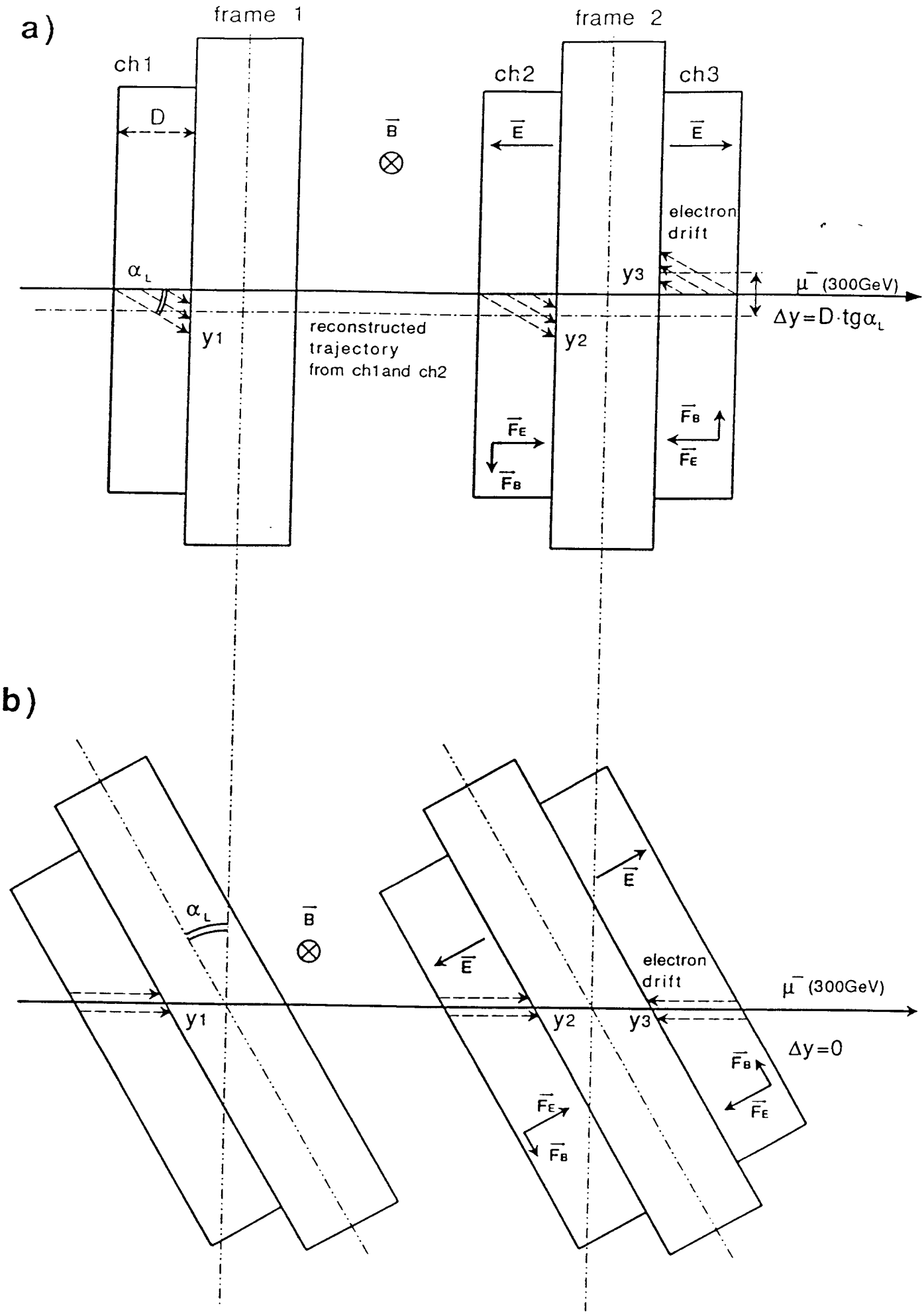

Figure 2 : Geometry of the chamber telescope. The Lorentz angle measurment is explained in (a), the compensation of the magnetic field effect in

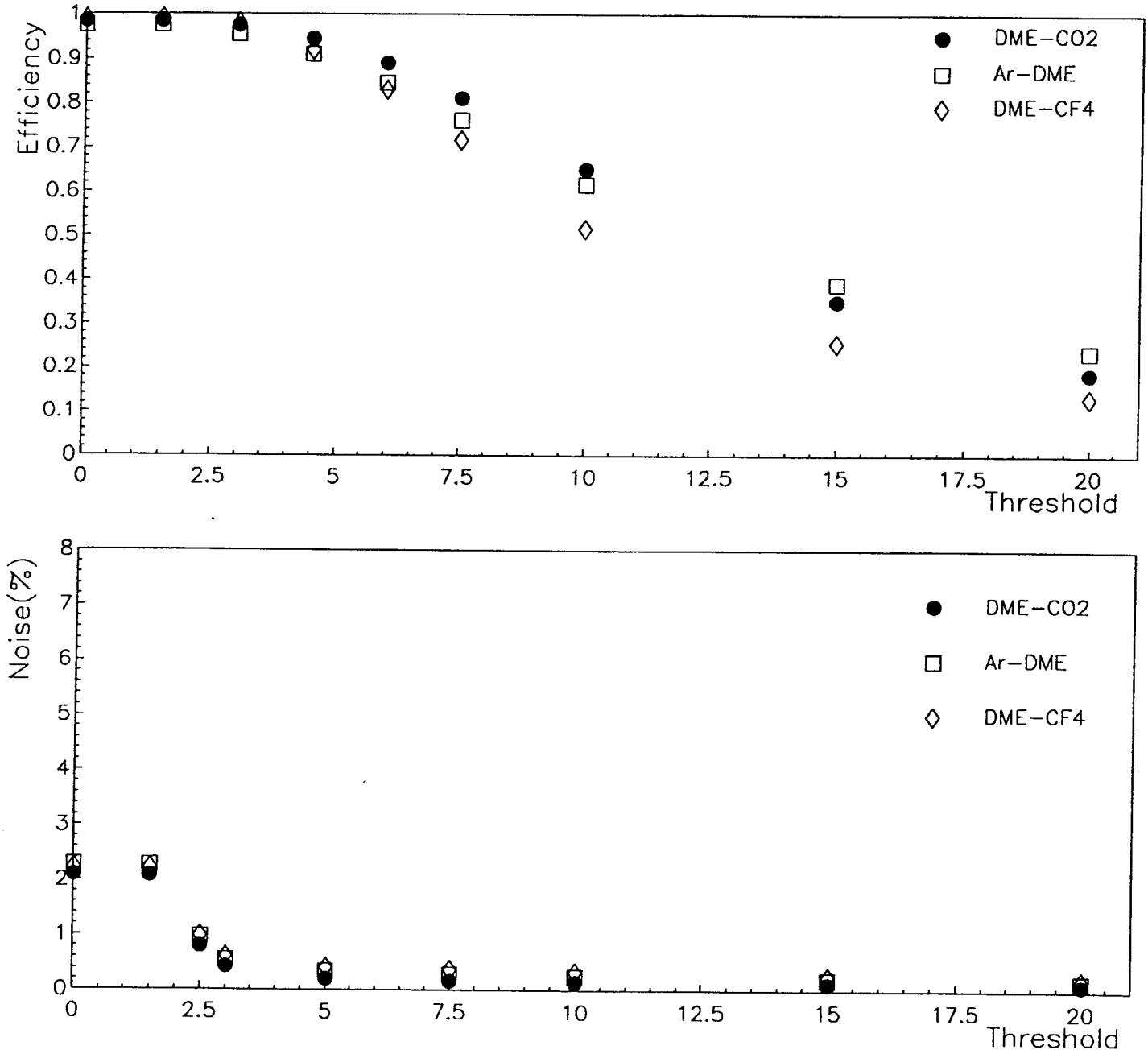

Figure 3 : Efficiency and noise occupation (proportion of hit strips) of chamber 2 as a function of the threshold, in case of the analogical analysis.The threshold is in unit of the mean value of the pedestal rms,this is the second level threshold applied to the cluster amplitude (see text).

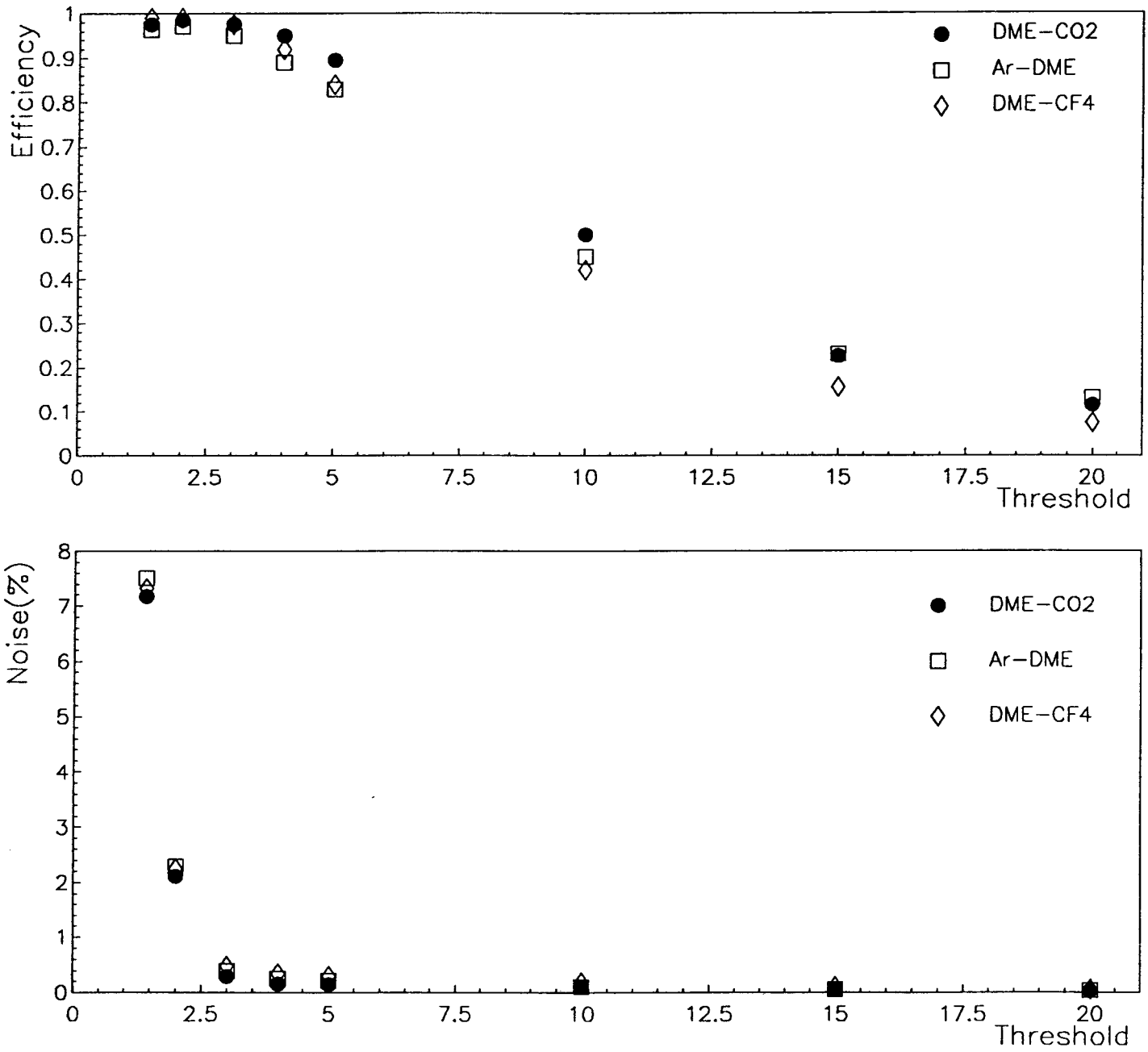

Figure 4 : Efficiency and noise occupation (proportion of hit strips) of chamber 2 as a function of the threshold, in case of the logical analysis.The threshold is in unit of the mean value of the pedestal rms,it is applied to the ADC amplitude of individual strips.

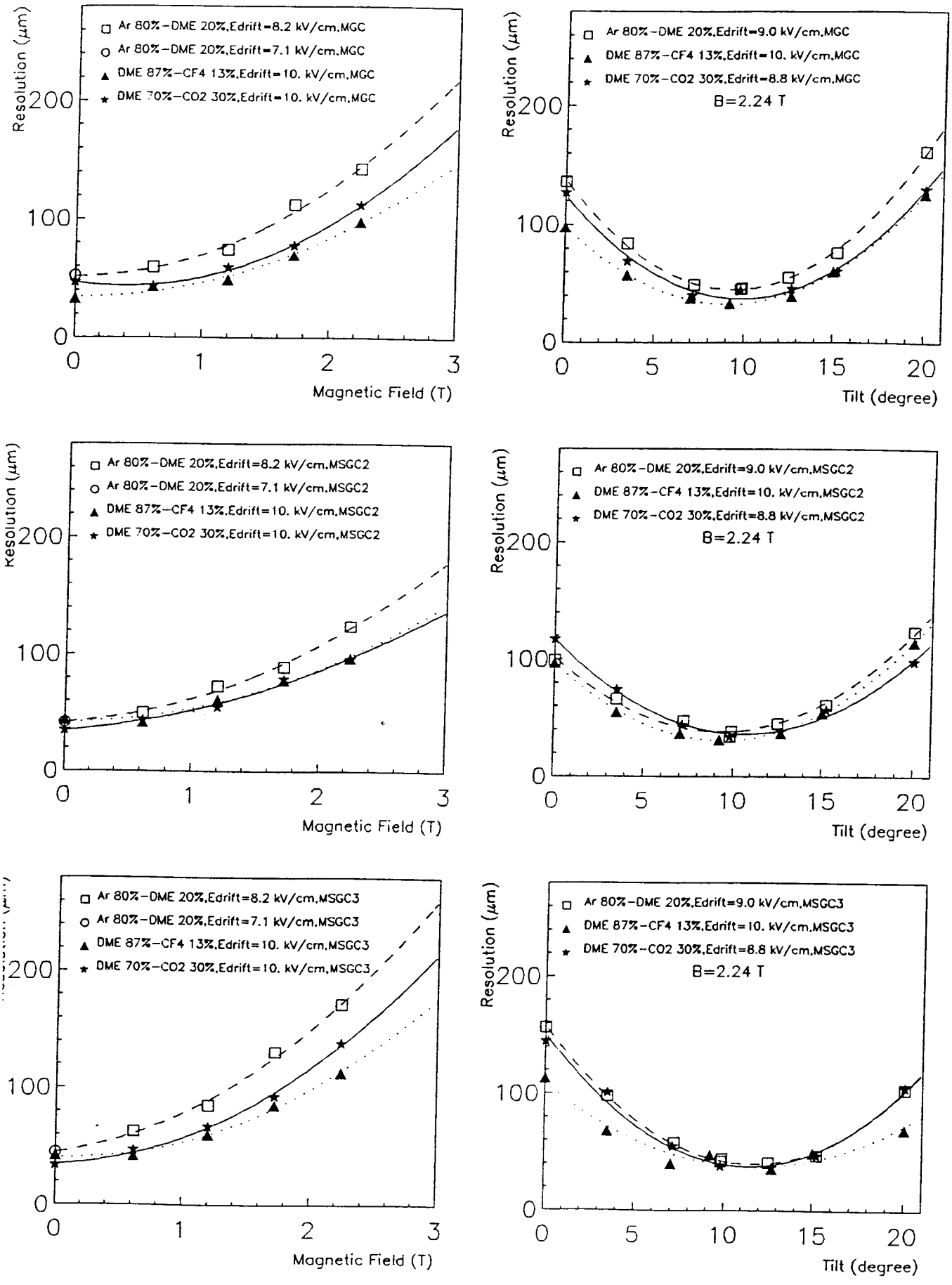

Figure 5 : Spatial resolutions estimated from the analogical analysis, versus magnetic field and versus tilt of the detectors. The various gas mixtures are compared.

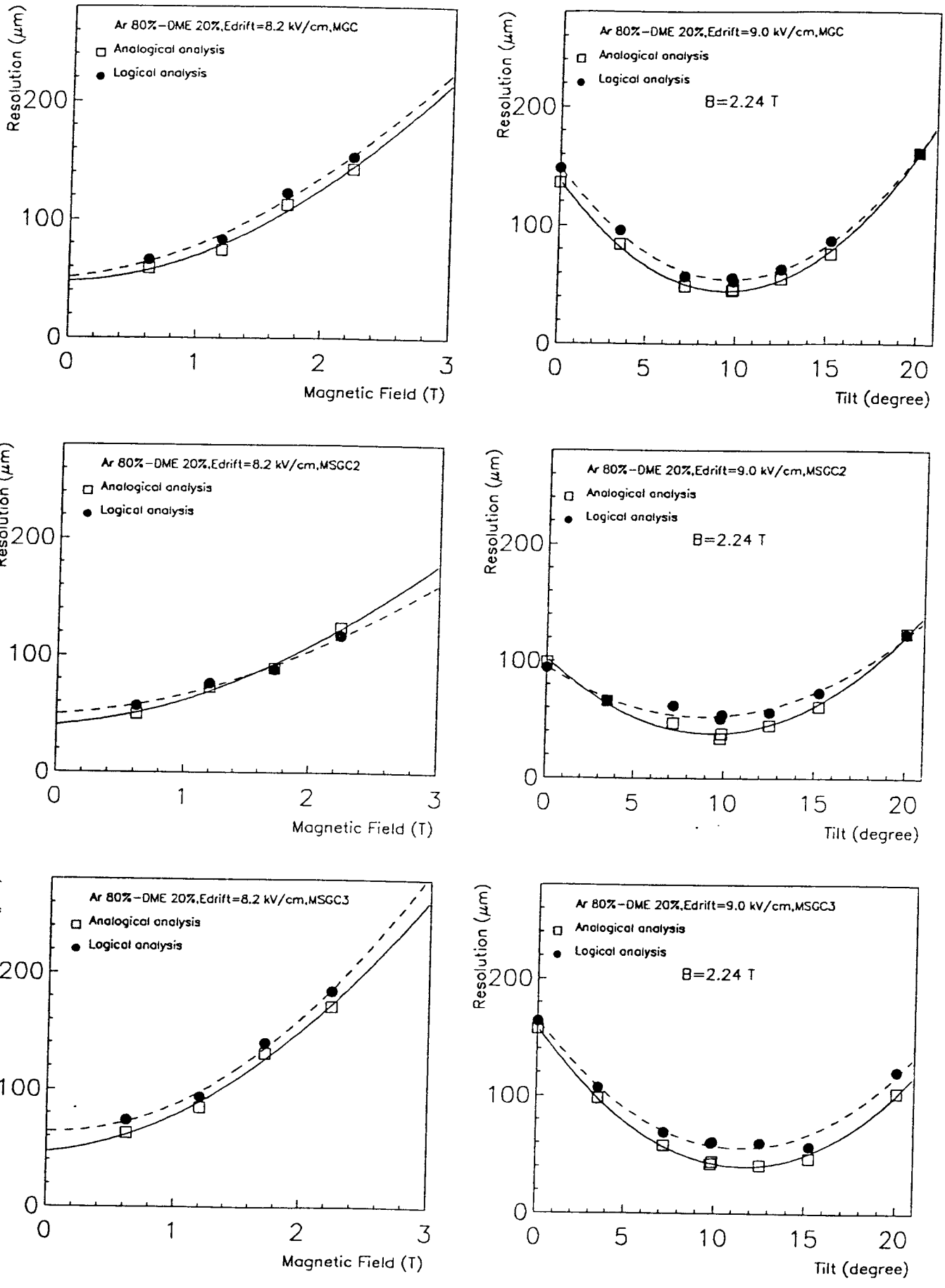

Figure 6.a : Comparison of the spatial resolutions obtained with the analogical and logical analyses for Ar 80%-DME 20% .

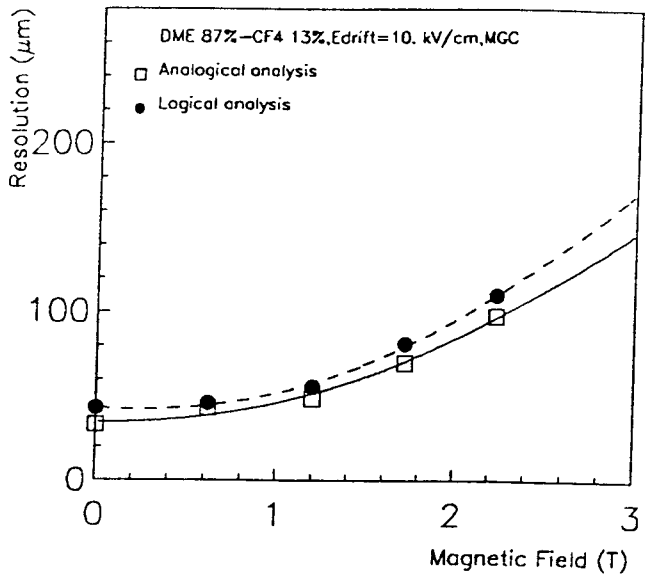

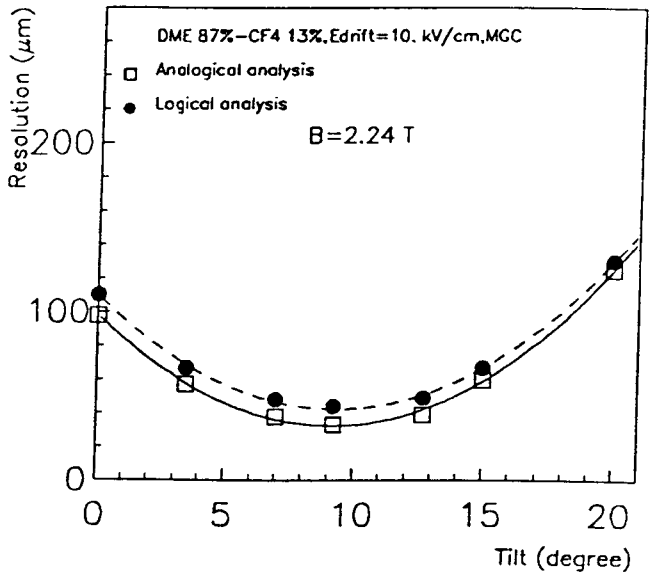

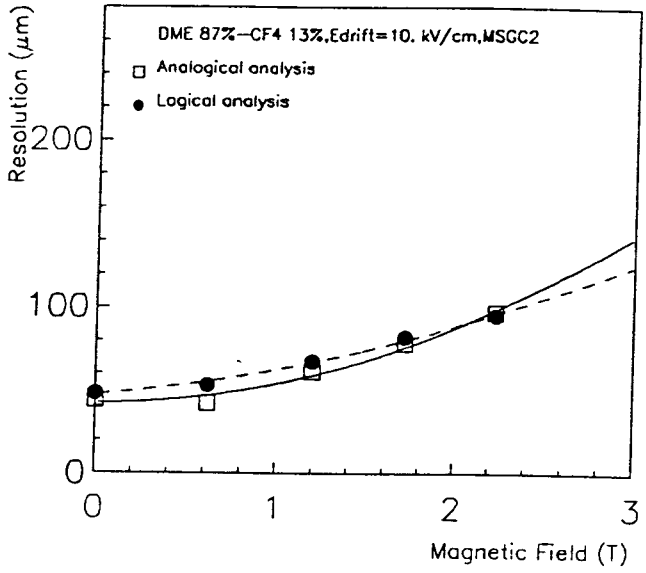

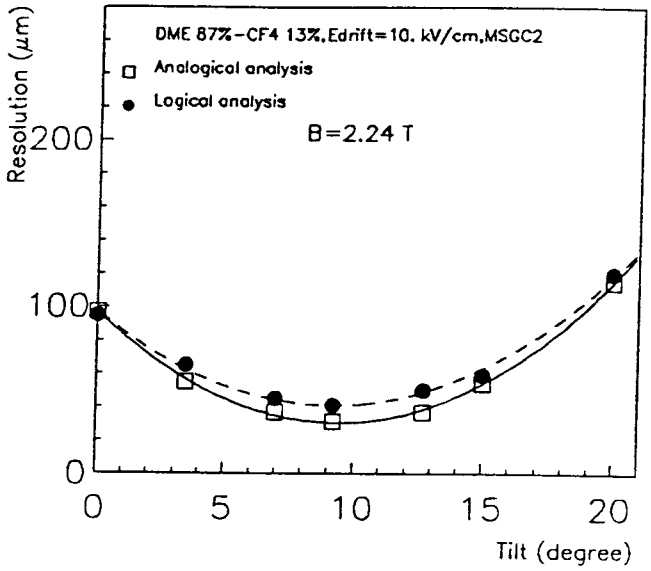

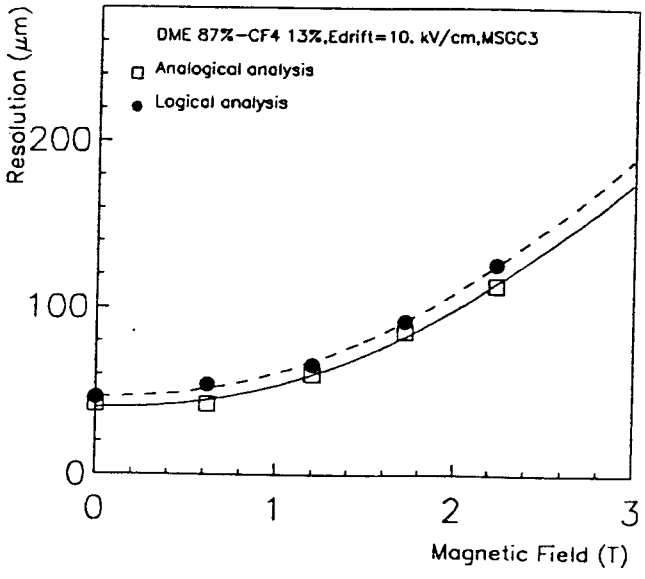

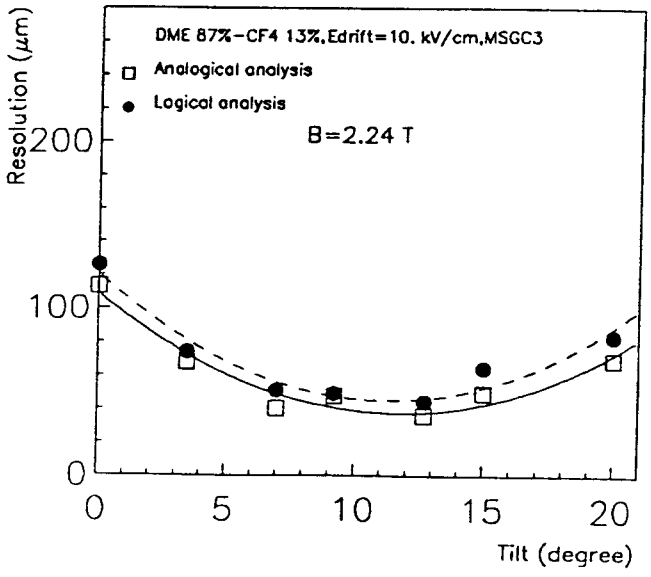

Figure 6.b : Comparison of the spatial resolutions obtained with the analogical and logical analyses for DME 87%-CF_4 13% .

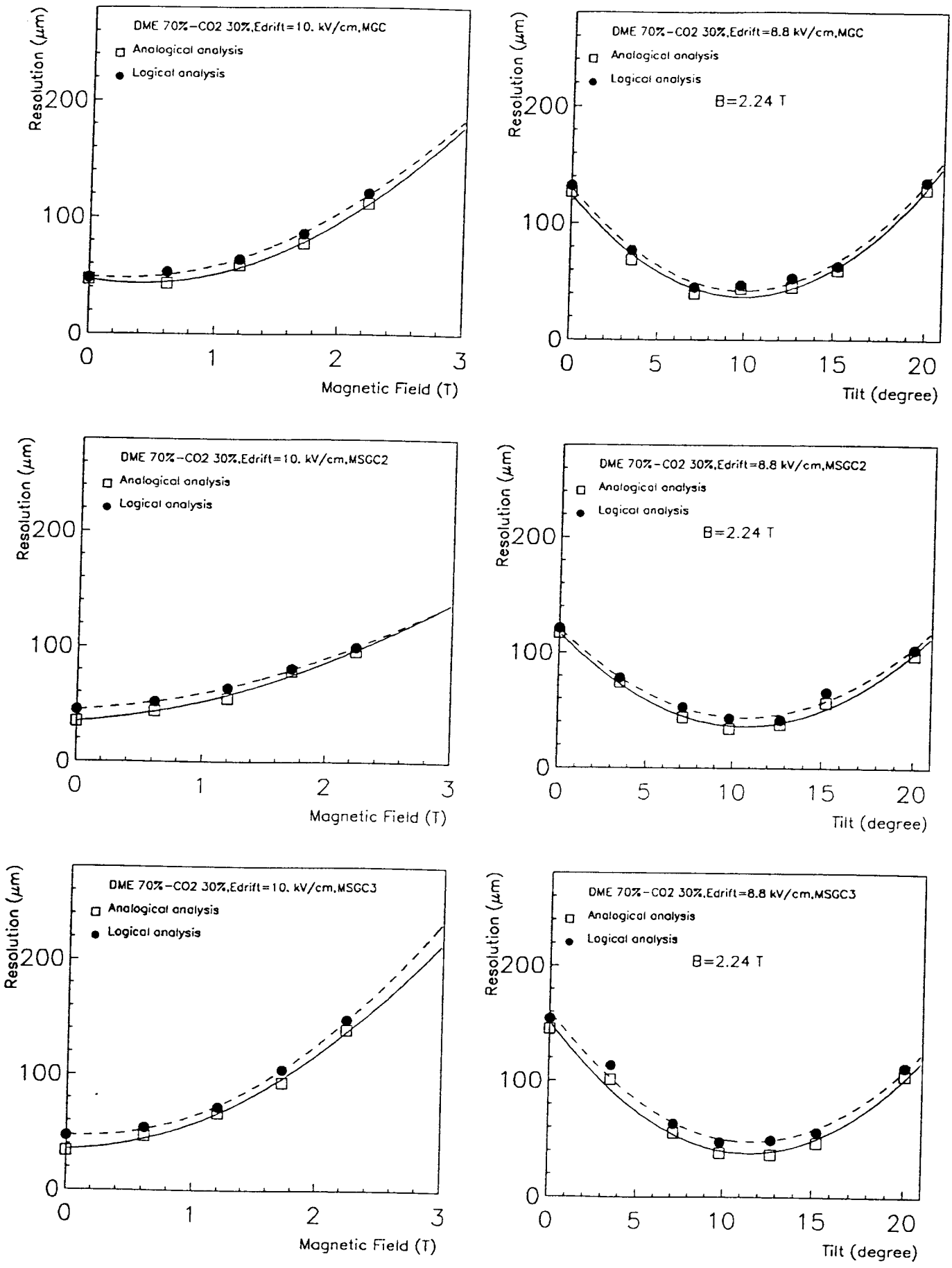

Figure 6.c : Comparison of the spatial resolutions obtained with the analogical and logical analyses for DME 70%-CO_2 30% .

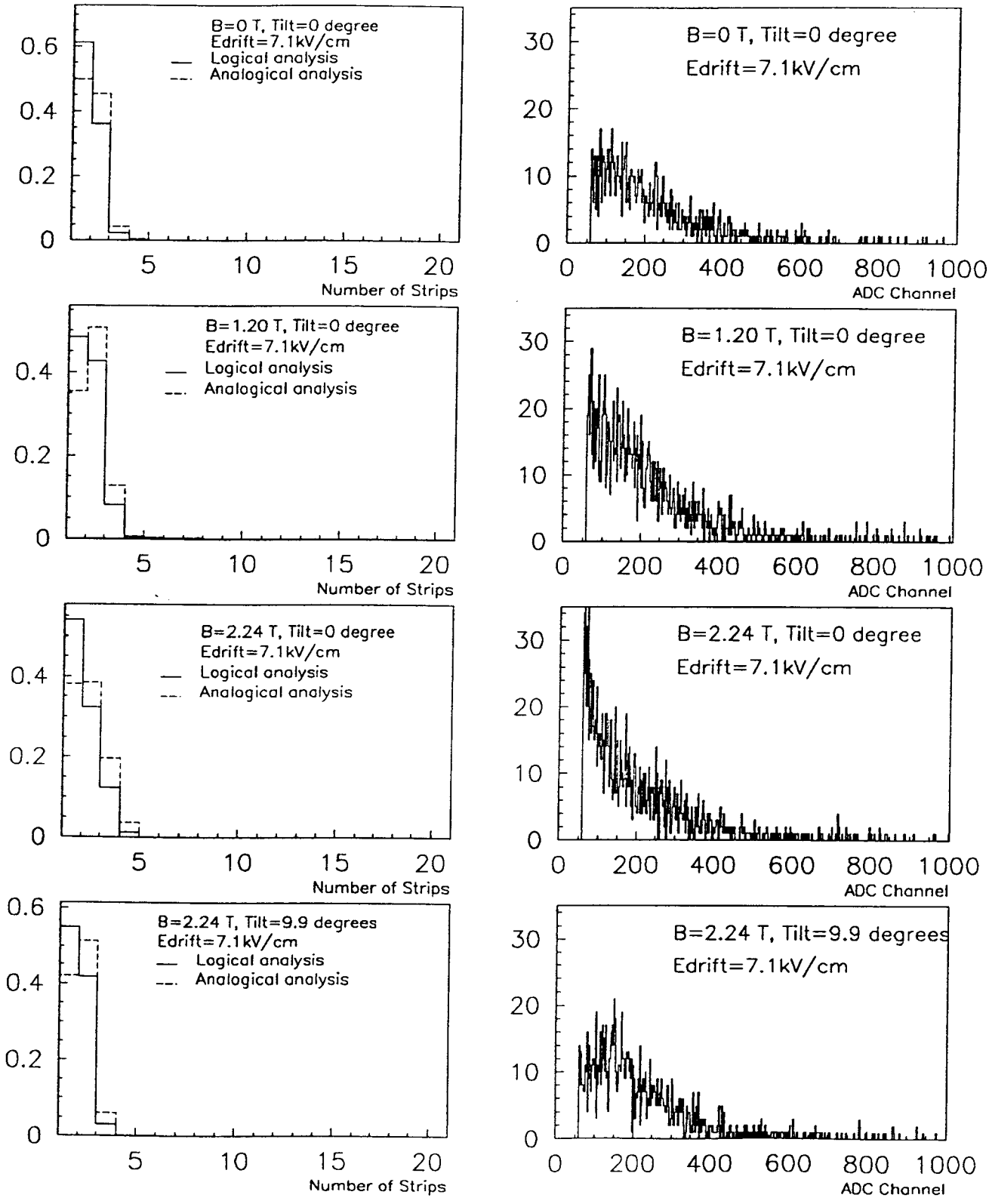

Figure 7.a : Distributions of the number of excited strips per cluster normalize to the total number of tracks. Distribution of the cluster height in arbitrary units for MGC for Ar 80%-DME 20% .

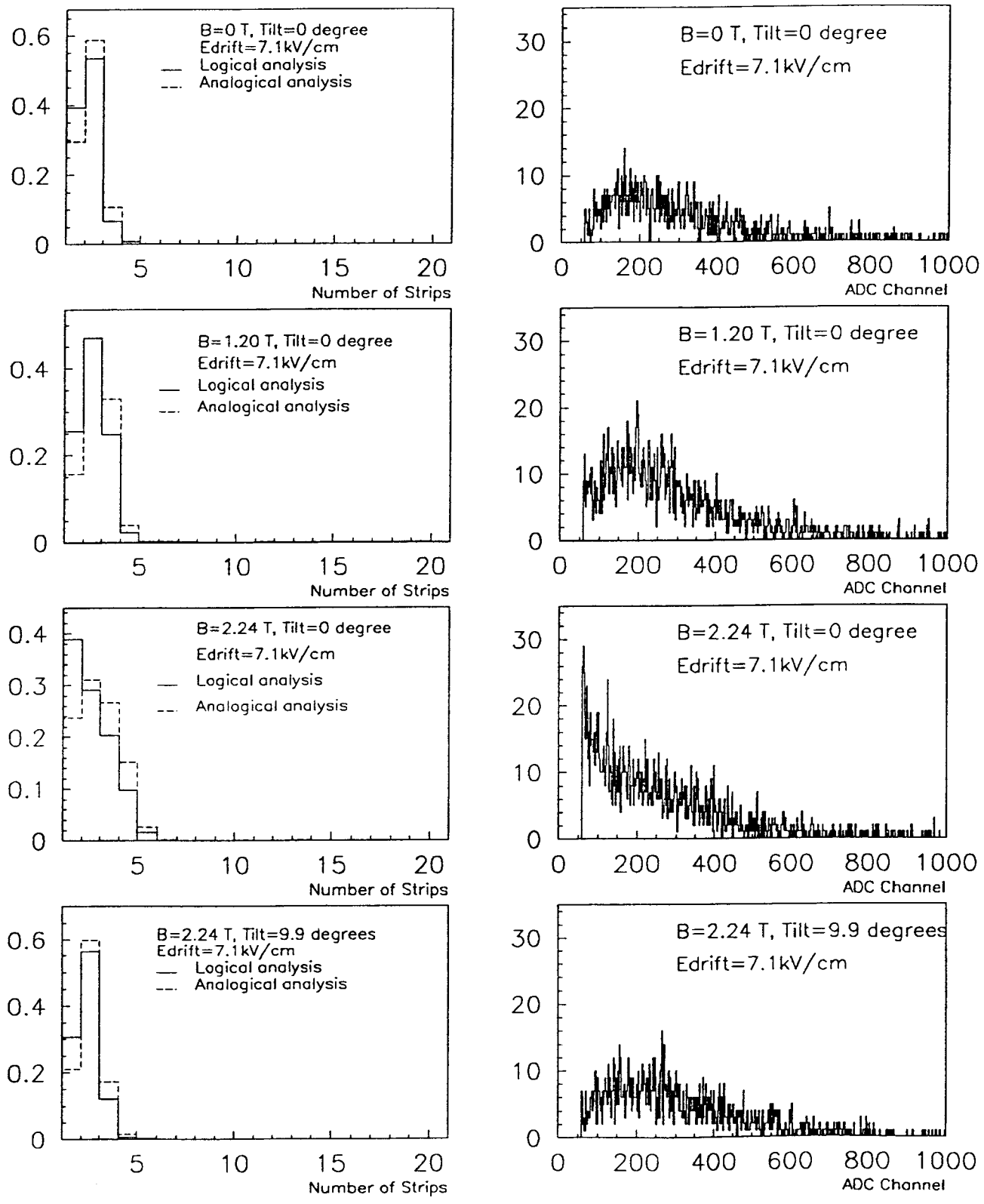

Figure 7.b : Distributions of the number of excited strips per cluster normalize to the total number of tracks. Distribution of the cluster height in

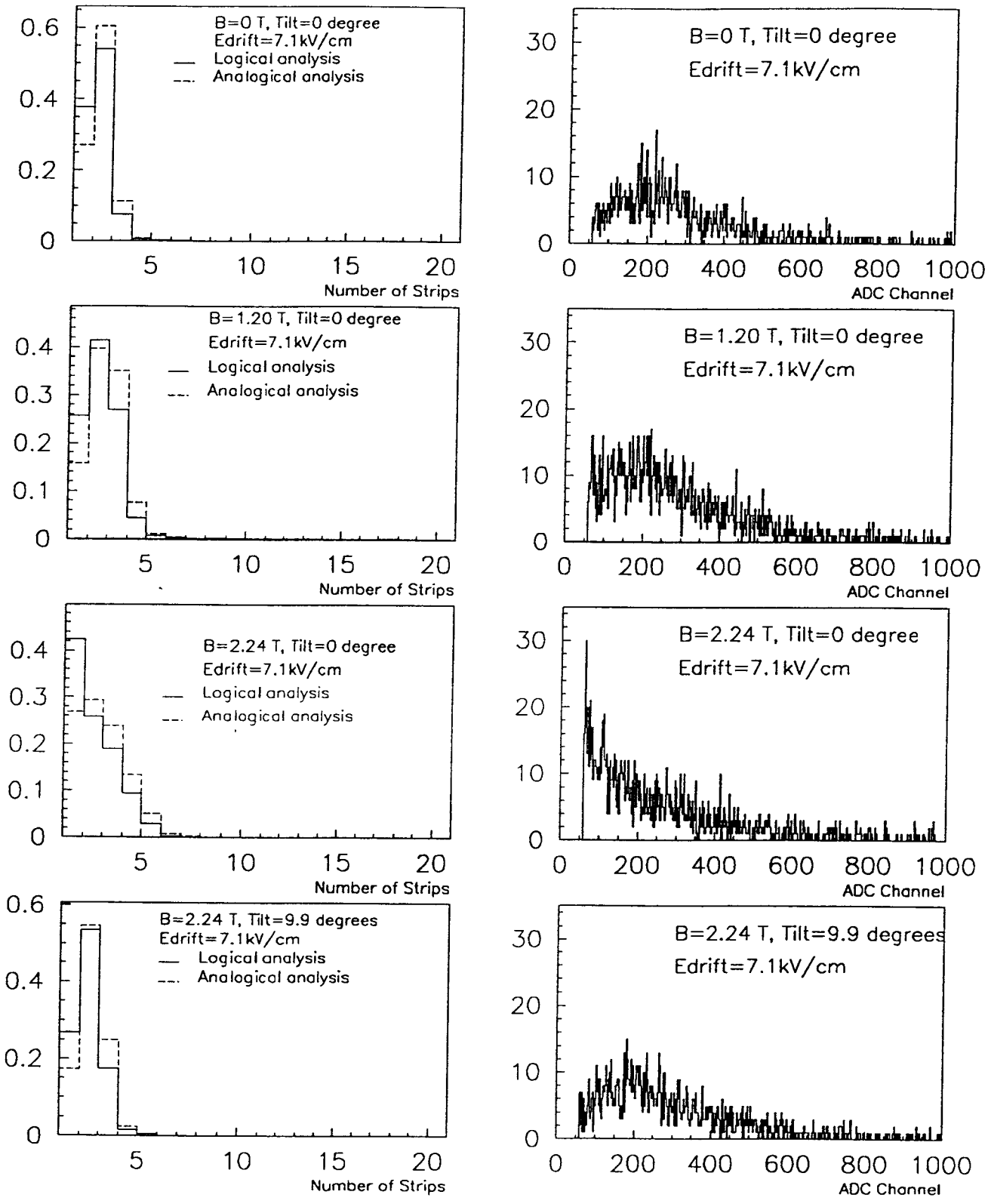

Figure 7.c : Distributions of the number of excited strips per cluster normalize to the total number of tracks. Distribution of the cluster height in arbitrary units for MSGC3 for Ar 80%-DME 20%

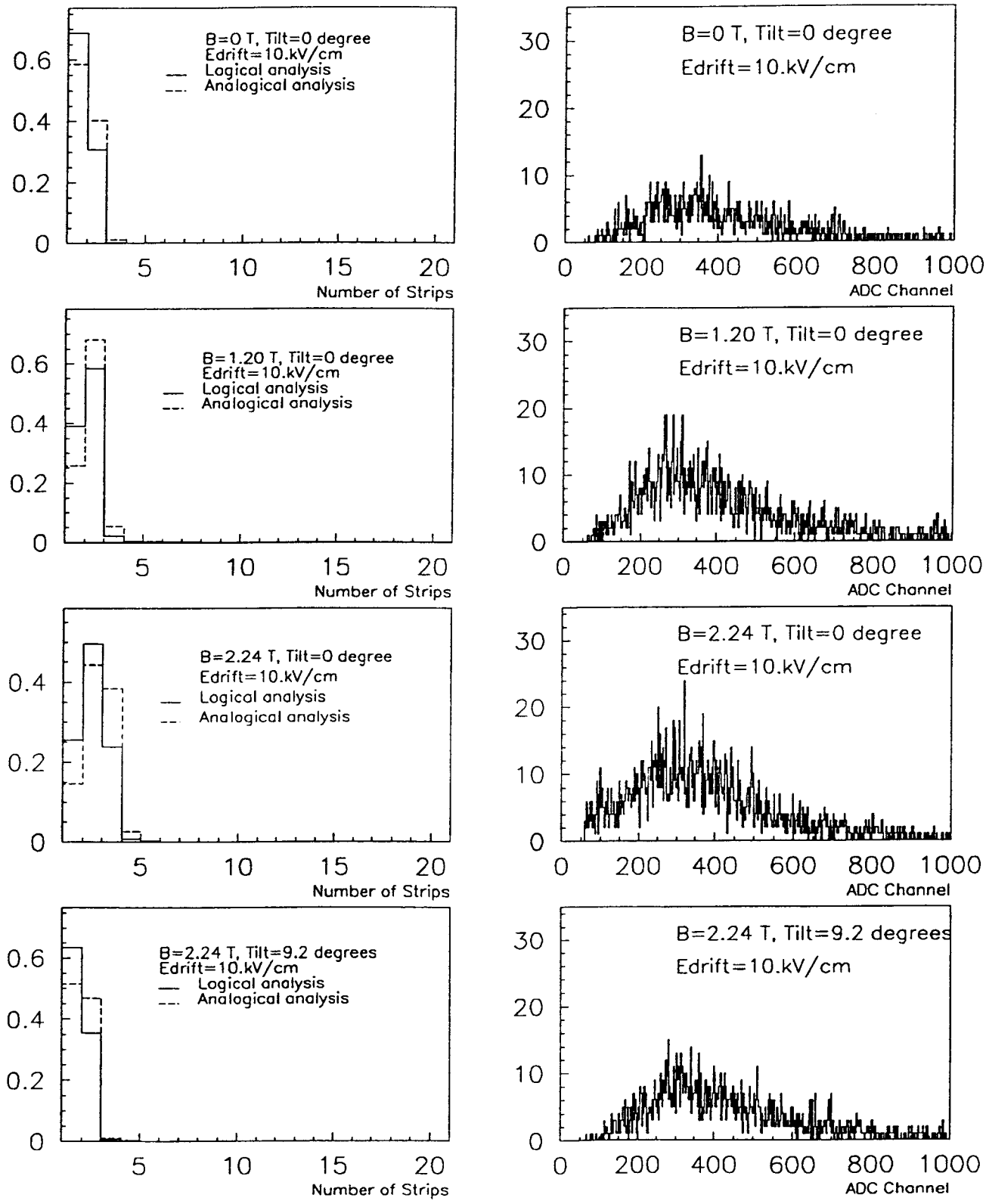

Figure 7.d : Distributions of the number of excited strips per cluster normalize to the total number of tracks. Distribution of the cluster height in arbitrary units for MGC for DME 87%-CF$_4$ 13%

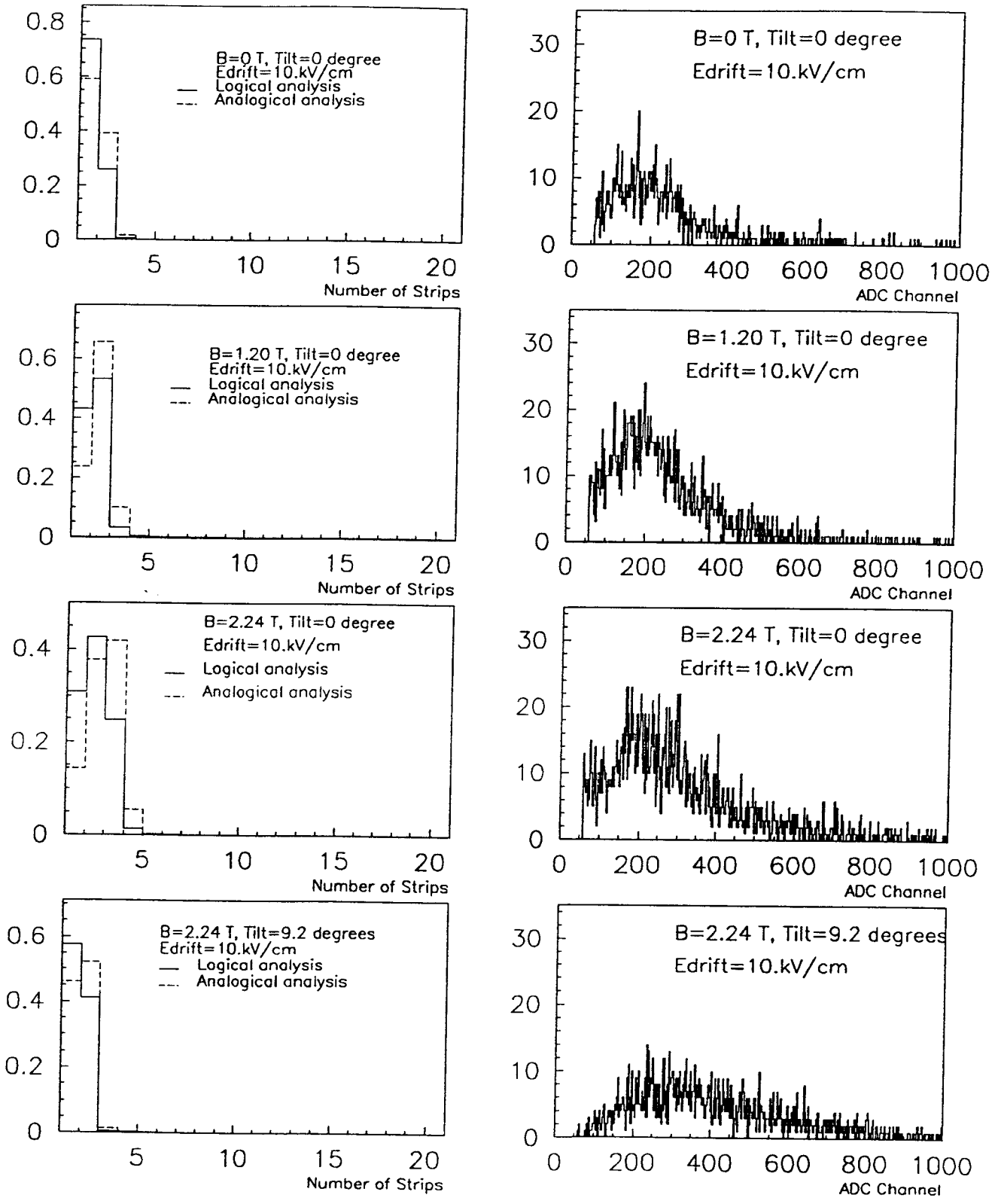

Figure 7.e : Distributions of the number of excited strips per cluster normalize to the total number of tracks. Distribution of the cluster height in arbitrary units for MSGC2 for DME 87%-CF_4 13% .

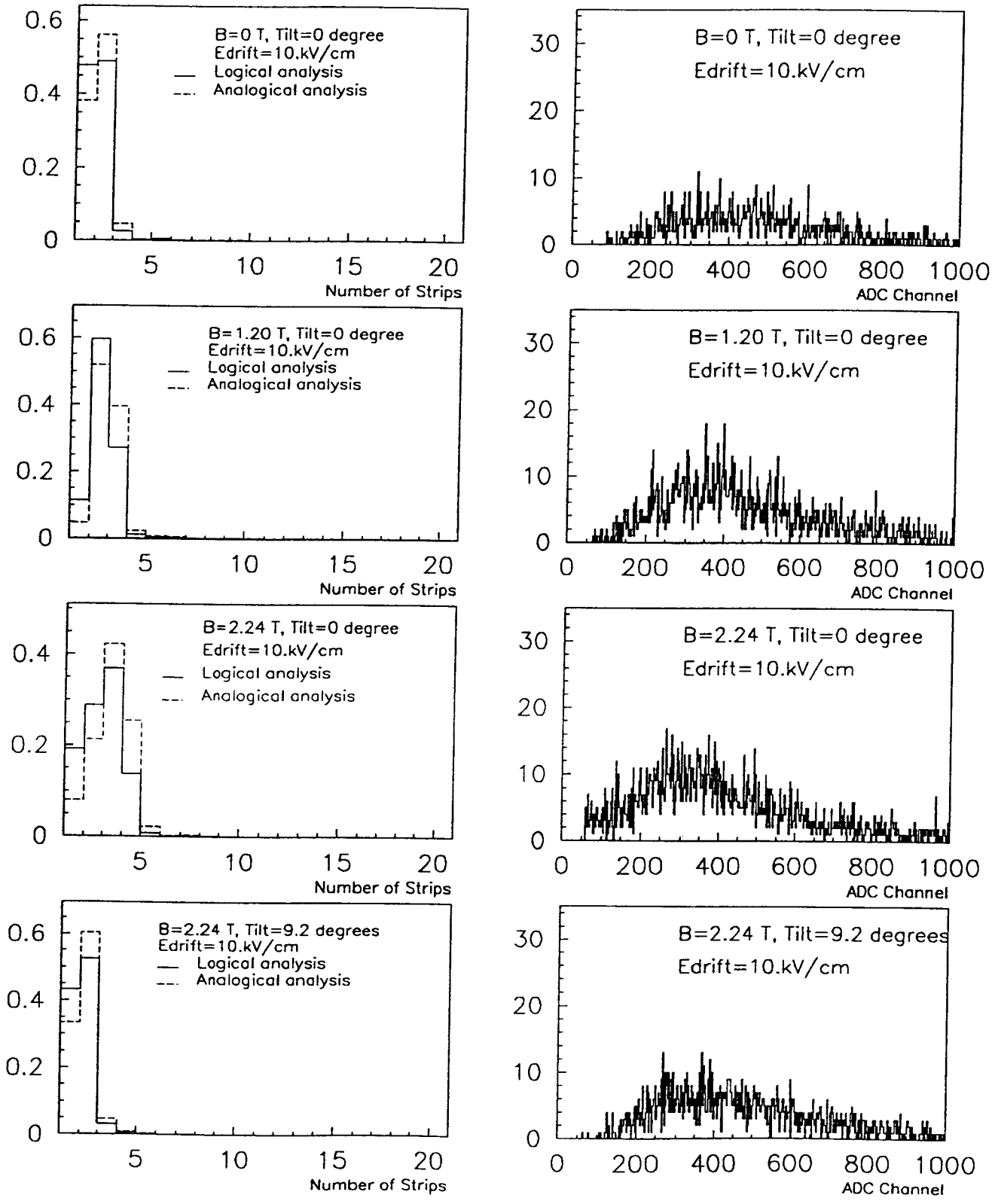

Figure 7.f : Distributions of the number of excited strips per cluster normalize to the total number of tracks. Distribution of the cluster height in arbitrary units for MSGC3 for DME 87%-CF_4 13% .

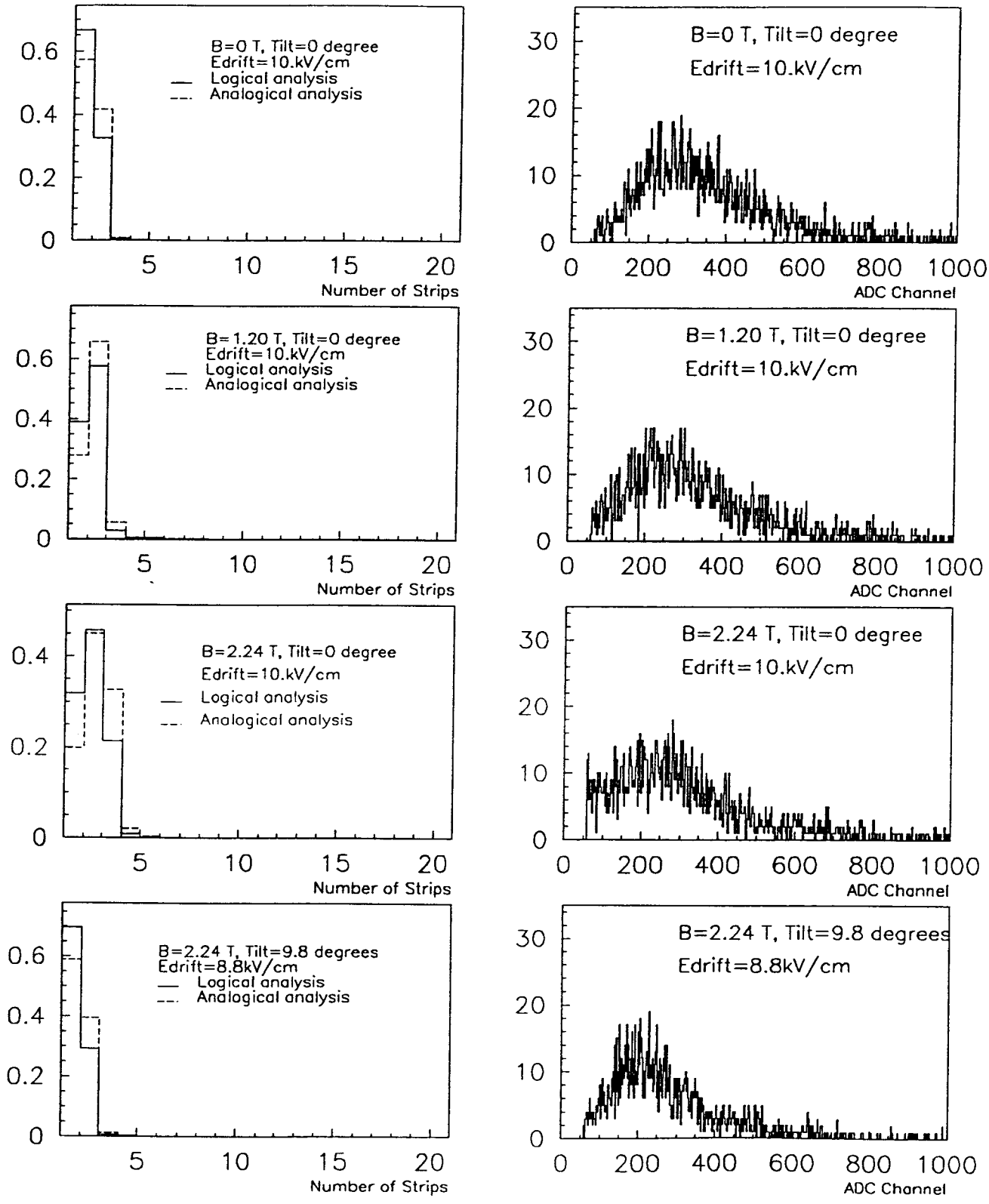

Figure 7.g : Distributions of the number of excited strips per cluster normalize to the total number of tracks. Distribution of the cluster height in arbitrary units for MGC for DME 70%-CO_2 30%

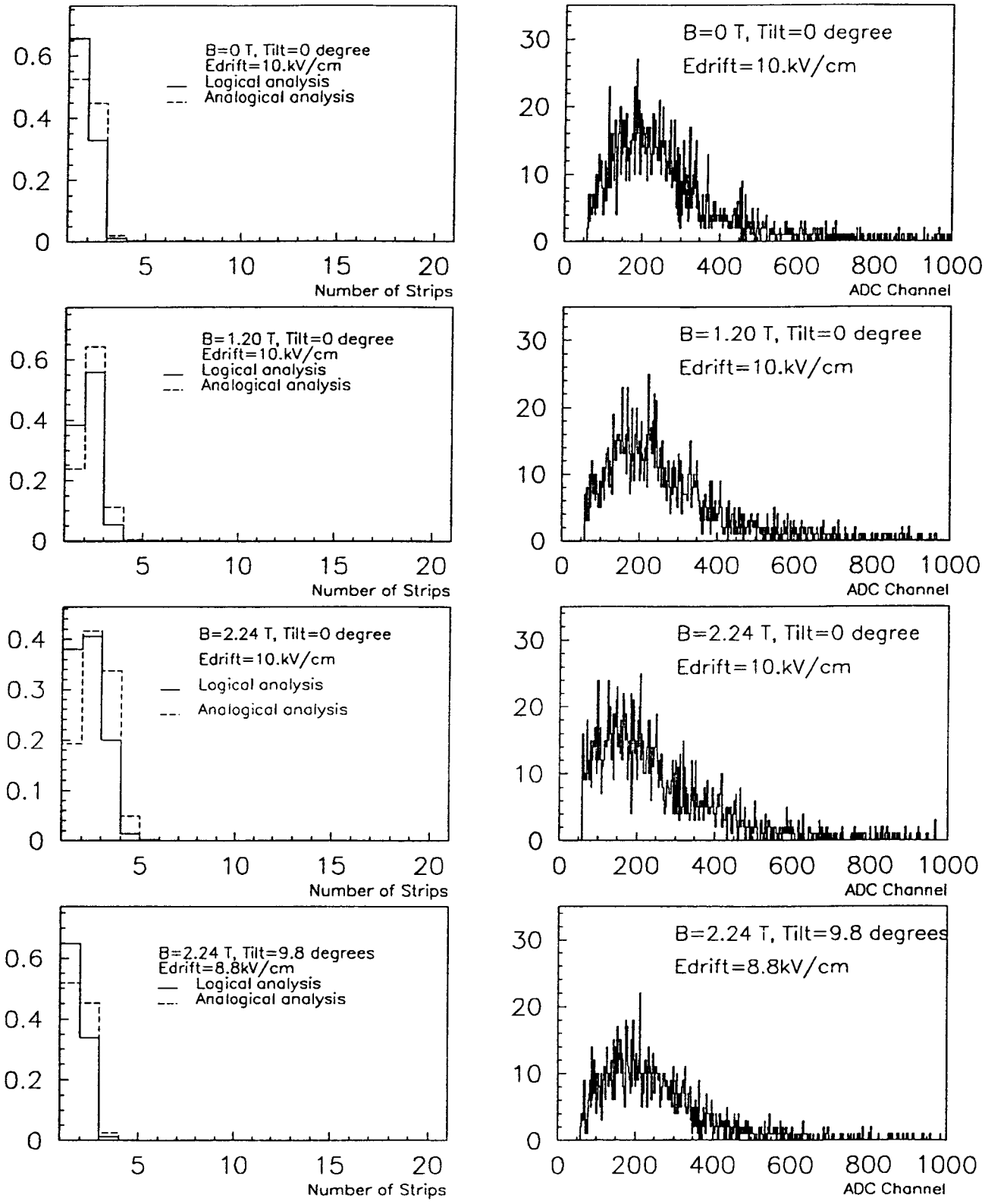

Figure 7.h : Distributions of the number of excited strips per cluster normalize to the total number of tracks. Distribution of the cluster height in arbitrary units for MSGC2 for DME 70%-CO_2 30% .

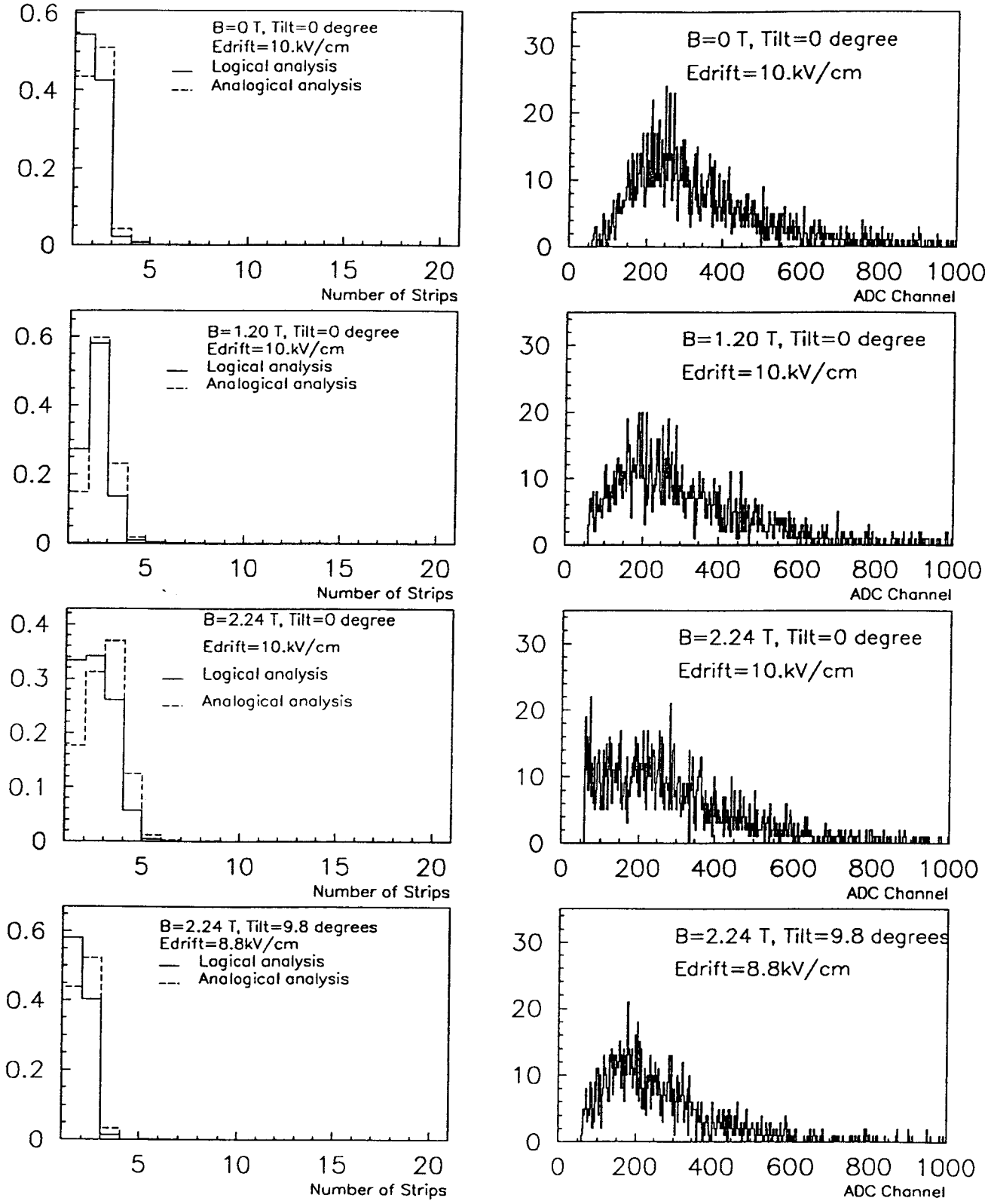

Figure 7.i : Distributions of the number of excited strips per cluster normalize to the total number of tracks. Distribution of the cluster height in arbitrary units for MSGC3 for DME 70%-CO_2 30% .

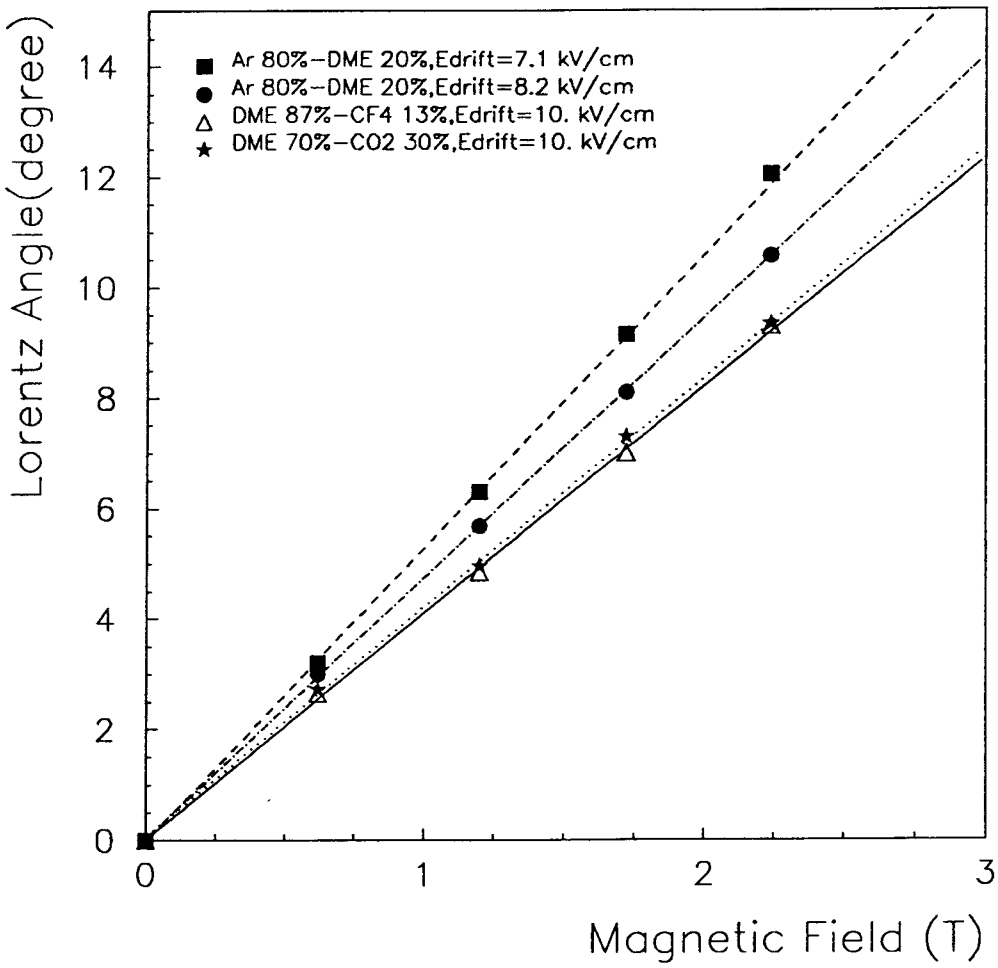

Figure 8 : Lorentz angle versus magnetic field for the various gas mixtures.

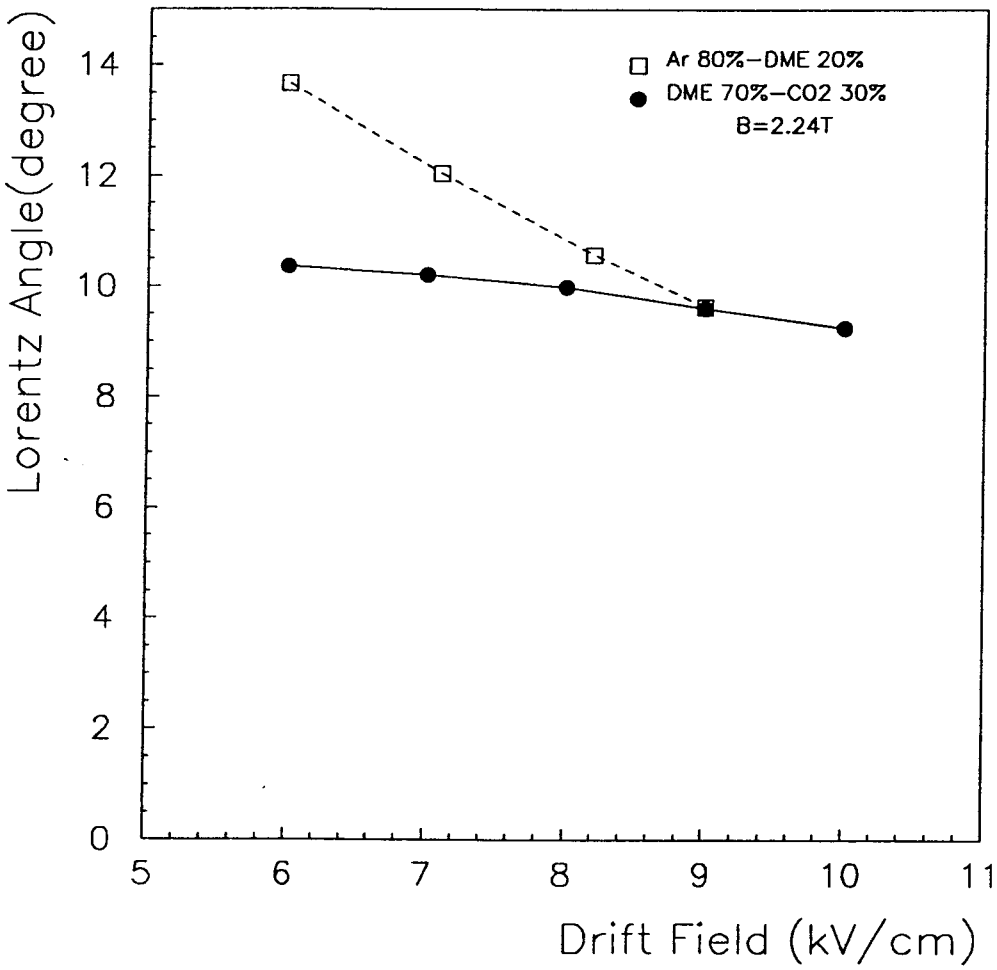

Figure 9 : Lorentz angle versus drift field at B=2.24T.

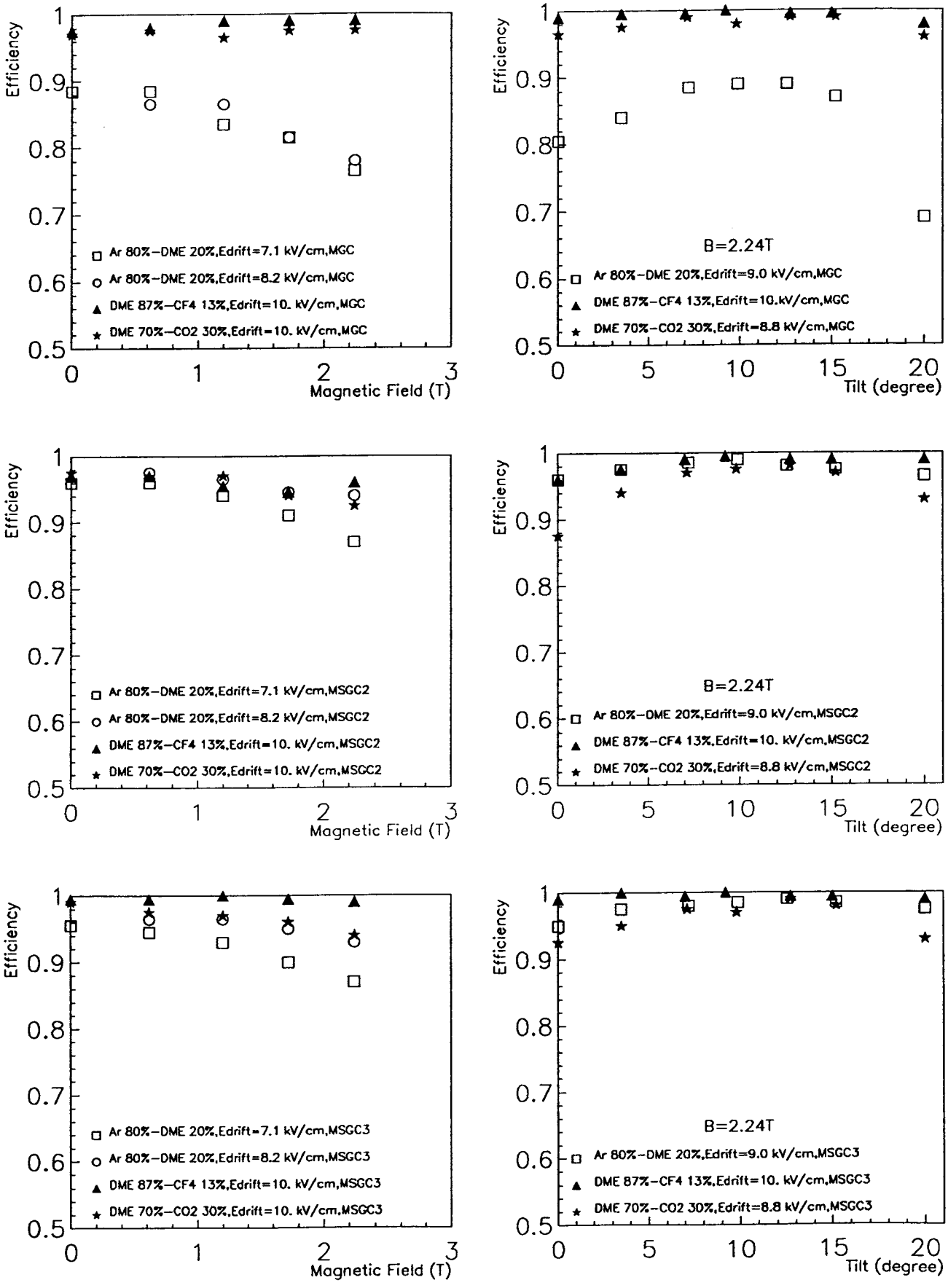

Figure 10 : Efficiencies estimated from the analogical analysis, versus magnetic field and versus tilt of the detectors. The various gas mixtures are

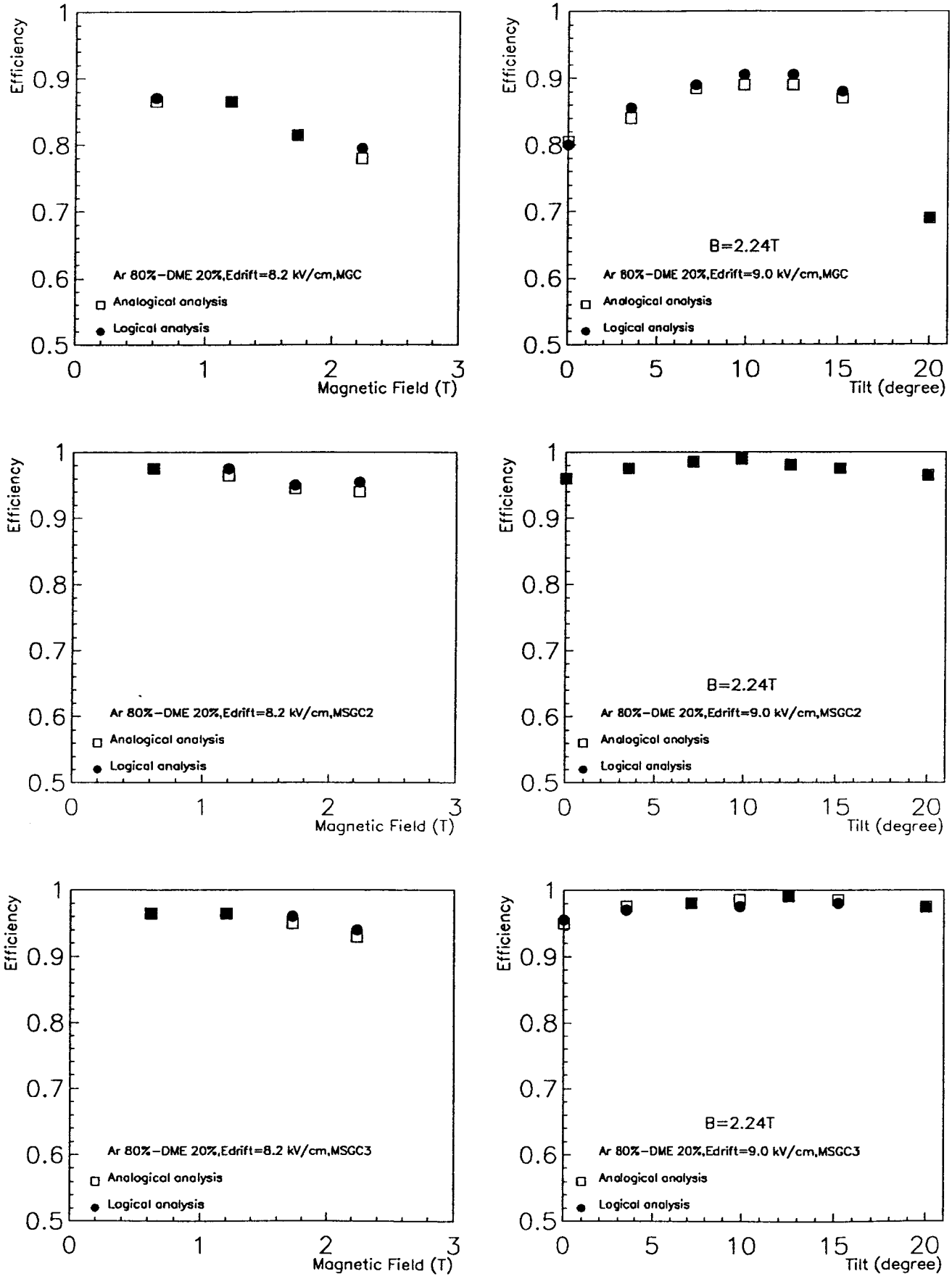

Figure 11.a : Comparison of the efficiencies obtained with the analogical and logical analyses for Ar 80%-DME 20% .

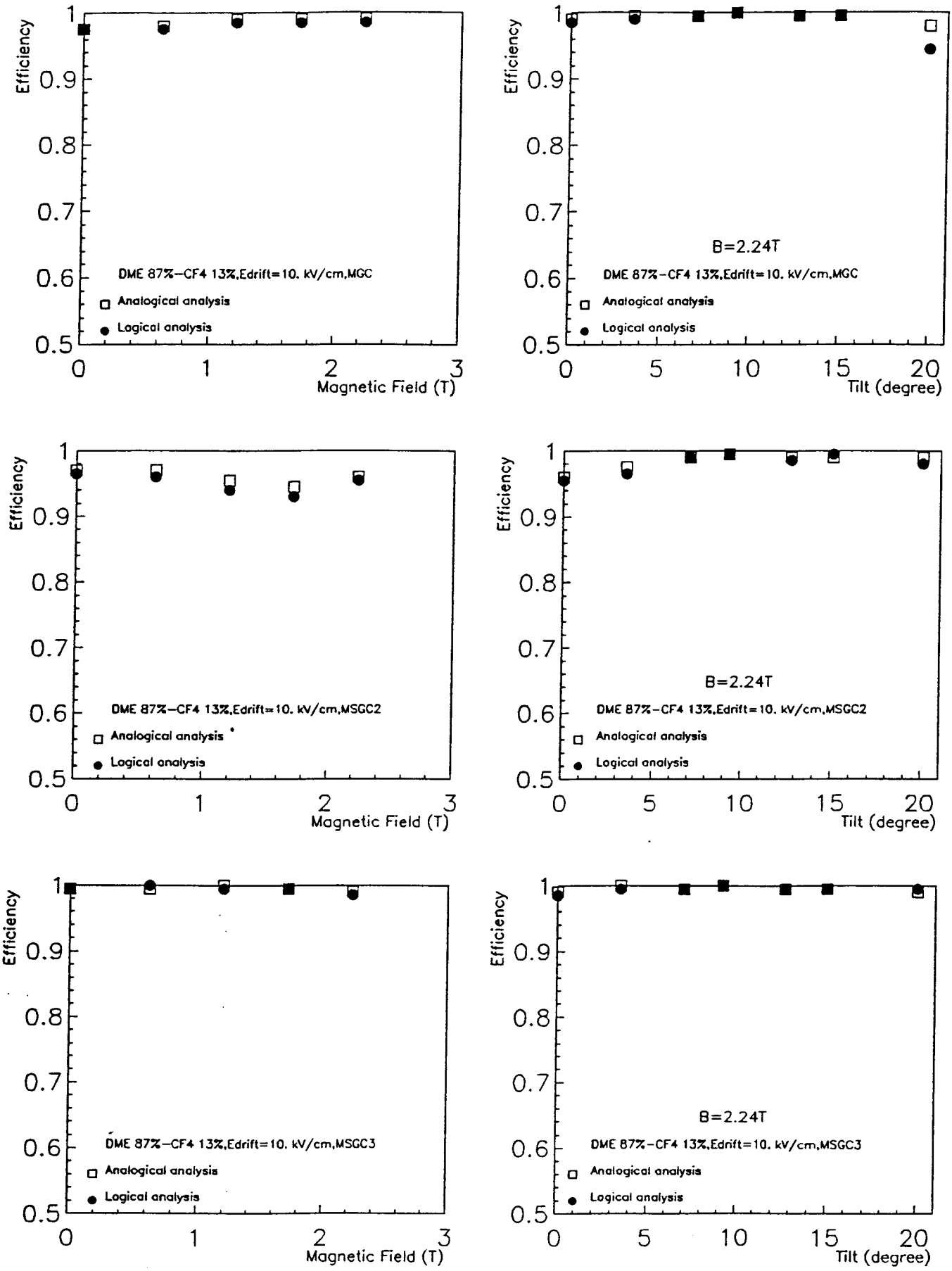

Figure 11.b : Comparison of the efficiencies obtained with the analogical and logical analyses for DME 87%-CF_4 13% .

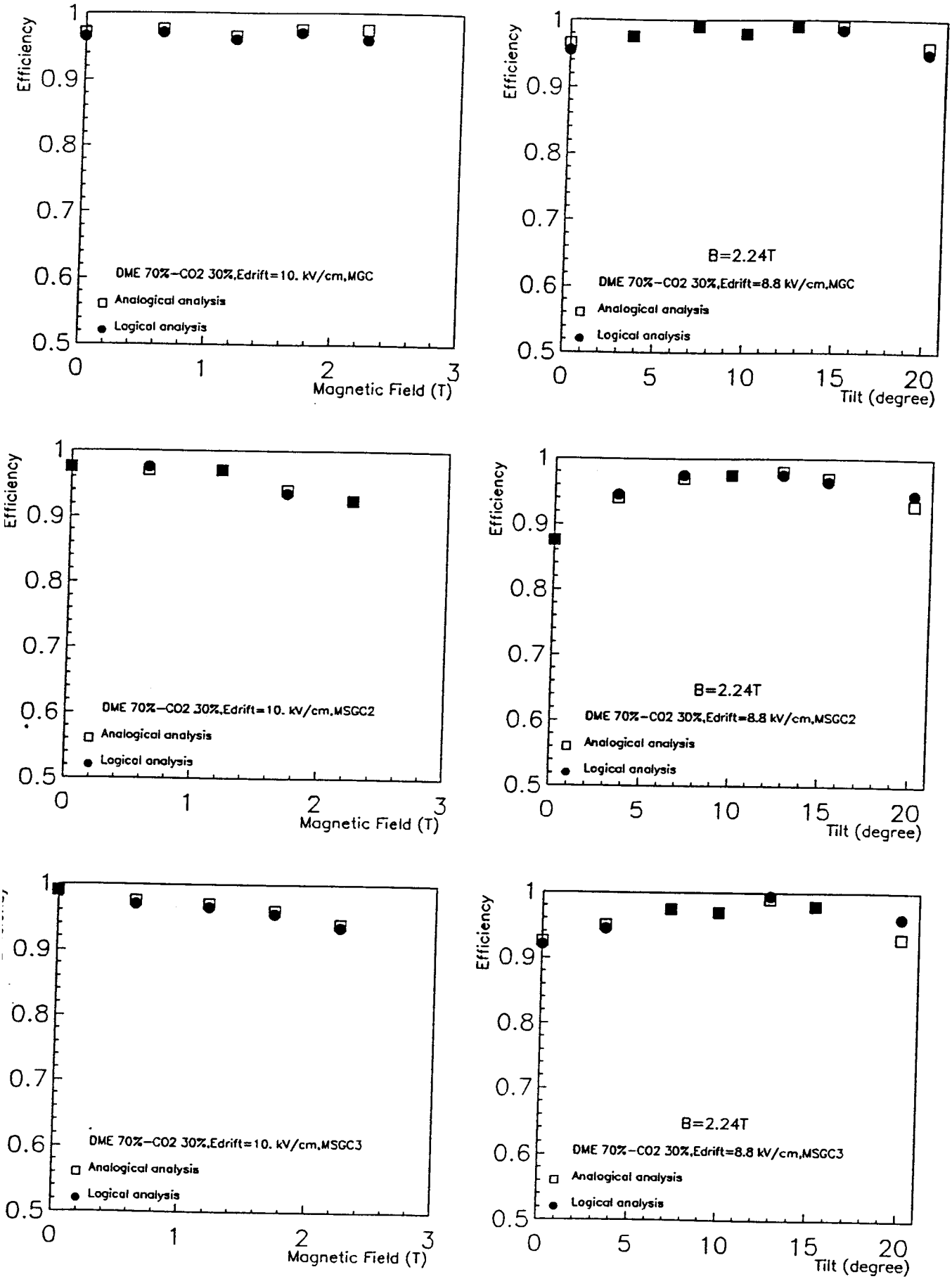

Figure 11.c : Comparison of the efficiencies obtained with the analogical and logical analyses for DME 70%-CO_2 30% .